17th World Conference on Earthquake Engineering, 17WCEE
Sendai, Japan - September 13th to 18th 2020

PROPOSAL OF SIMPLIFIED CHARACTERIZATION METHOD OF PULSE-LIKE GROUND MOTIONS

M. Sugino [(1)], K. Tanaka [(2)], Y. Hayashi [(3)]

[(1)] *Associate Professor, Kyoto University, rp-sugino@archi.kyoto-u.ac.jp*
[(2)] *Ph.D. student, Kyoto University, rp-tanaka@archi.kyoto-u.ac.jp*
[(3)] *Professor, Kyoto University, hayashi@archi.kyoto-u.ac.jp*

Abstract

Pulse-like ground motions have caused severe damage to buildings. Such pulse-like ground motions were observed in the 1994 Northridge earthquake, the 1995 Kobe earthquake, the 1999 Chi-Chi earthquake and so on. In the 2016 Kumamoto earthquake in Japan, large-amplitude pulse-like ground motions which had several predominant periods were observed. To confirm aseismic performance of buildings against such strong pulse-like ground motions, it is effective to characterize the pulse-like ground motions by simple pulse-like waveforms which consist of several parameters. This is because we can easily understand which parameters of the pulse-like waveforms affect the response of buildings.

Therefore, Sugino et al. (2018) have established a simplified characterization method of observed pulse-like ground motions by Gabor wave. Gabor wave is represented by the product of harmonic wave and Gauss function. Gabor wave is defined by pulse characteristic parameters; pulse period, velocity amplitude and wave number. The proposed characterized method in Sugino et al. (2018) uses pseudo-velocity response spectra ${}_pS_v$ and concentration ratio of energy of observed ground motions. The concentration ratio of energy is the ratio of total input energy spectra to momentary input energy spectra. It is difficult to say that this characterized method is simple enough because the calculation of the momentary input energy spectra is complicated in some degree.

In this study, we improve the simplified characterization method to use only pseudo-velocity response spectra ${}_pS_v$. In our new proposed characterization method, only the maximum value of the pseudo-velocity response spectra ${}_pS_v$ at different damping ratios and the period at the maximum ${}_pS_v$ of the observed pulse-like ground motions are needed. The pulse characteristic parameters are obtained by substituting the maximum ${}_pS_v$ and the period into the evaluation equations which are proposed in this paper. The evaluation equations proposed in this paper are developed based on the response spectrum characteristics of Gabor wave.

In addition, we apply the characterization method to several typical pulse-like ground motions observed all over the world and calculate the pulse characteristic parameters of the ground motions. It is confirmed that the velocity waveforms and the response spectra of the characterized Gabor wave approximately coincide with those of the observed ground motions.

The advantages of the characterization method proposed in this paper are as follows. Anyone can easily calculate the pulse characteristic parameters as long as the response spectrum is obtained because this method does not use any complicated processing such as calculating momentary input energy as our previous method, integration of accelerations, Fourier transform or Wavelet transform. In this method, the same pulse characteristic parameters can be obtained regardless of users because we do not have to determine the pulse characteristic parameters by trial and error. Furthermore, even for pulse-like ground motions which have several pulse periods such as the ground motions observed during the 2016 Kumamoto earthquake, this method can determine multiple pulse characteristic parameters.

Keywords: pulse-like ground motion; characterization; response spectrum; pulse period

1. Introduction

Pulse-like ground motions have caused severe damage to buildings. Such pulse-like ground motions were observed in the 1994 Northridge earthquake, the 1995 Kobe earthquake, the 1999 Chi-Chi earthquake and so on. In the 2016 Kumamoto earthquake in Japan, large-amplitude pulse-like ground motions which had several predominant periods were observed. To confirm aseismic performance of buildings against such strong pulse-like ground motions, it is effective to characterize the pulse-like ground motions by simple pulse-like waveforms which consist of several parameters. This is because we can easily understand which parameters of the pulse-like waveforms affect the response of buildings.

Therefore, Sugino et al. (2018) [1] have established a simplified characterization method of observed pulse-like ground motions by Gabor wave. Gabor wave is represented by the product of harmonic wave and Gauss function. Gabor wave is defined by pulse characteristic parameters; pulse period, velocity amplitude and wave number. The proposed characterized method in Sugino et al. (2018) uses pseudo-velocity response spectra ${}_pS_v$ and concentration ratio of energy of observed ground motions. The concentration ratio of energy is the ratio of total input energy spectra to momentary input energy spectra. It is difficult to say that this characterized method is simple enough because the calculation of the momentary input energy spectra is complicated in some degree.

In this study, we improve the simplified characterization method to use only pseudo-velocity response spectra ${}_pS_v$. In our new proposed characterization method, only the maximum value of the pseudo-velocity response spectra ${}_pS_v$ at different damping ratios and the period at the maximum ${}_pS_v$ of the observed pulse-like ground motions are needed. The pulse characteristic parameters are obtained by substituting the maximum ${}_pS_v$ and the period into the evaluation equations which are proposed in this paper. The evaluation equations proposed in this paper are developed based on the response spectrum characteristics of Gabor wave.

In this paper, first, the basic properties of Gabor wave used for our characterization method is described in chapter 2. Next, a propose simplified characterization method is explained in chapter 3. Chapter 4 describes the deriving process of the proposed evaluation equations for the characterization method. Finally, chapter 5 shows the results of applying the proposed characterization method to typical pulse-like ground motions observed all over the worlds as application examples of the proposed characterization method.

2. Gabor wave

Gabor wave in this study is represented by the product of the harmonic wave and the Gauss function based on [2]. The velocity waveform of the Gabor wave in this paper is defined by Eq. (1) to (3).

$$\dot{y}_0(t) = V \cdot \exp\left\{-\left(\frac{2\pi}{T_H}\cdot\frac{t'}{\sigma}\right)^2\right\}\cdot\cos\left(\frac{2\pi}{T_H}\cdot t'\right) \tag{1}$$

$$t' = t - 3\sigma / \left(2\pi / T_H\right) \tag{2}$$

$$\sigma = k\pi/3 \tag{3}$$

Here, t is time, T_H is harmonic wave period, V is velocity amplitude, and k is wave number.

Figure 1 shows the time history of Gabor wave whose wave number k is changed. Here, the velocity amplitude V = 1 and the harmonic wave period T_H = 1. Figure 2 shows acceleration response spectra S_a, pseudo velocity response spectra ${}_pS_v$ and displacement response spectra S_d with damping ratio h = 0.05 of Gabor wave whose wave number k is changed. Here, V = 1 and T_H = 1. Note that T is the period of the spectra. As can be seen in the figures, the amplitude of the spectra increases as k increases. The predominant periods of the spectra change to the short period from T_H when k is small.

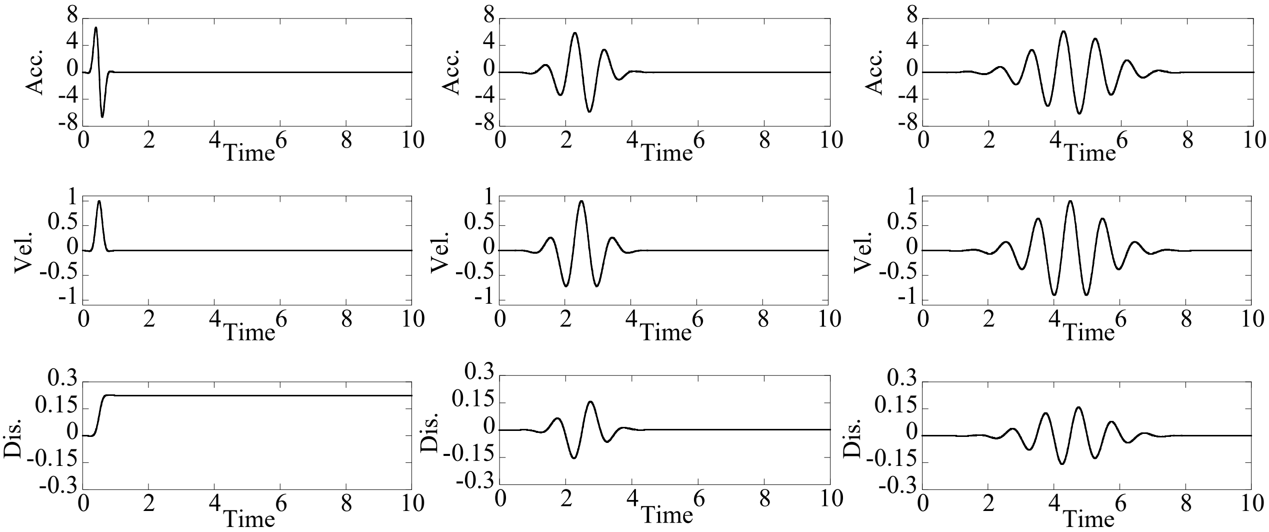

(a) k=1 (b) k=5 (c) k=9

Fig. 1 – Time history of Gabor wave (V=1, T_H =1)

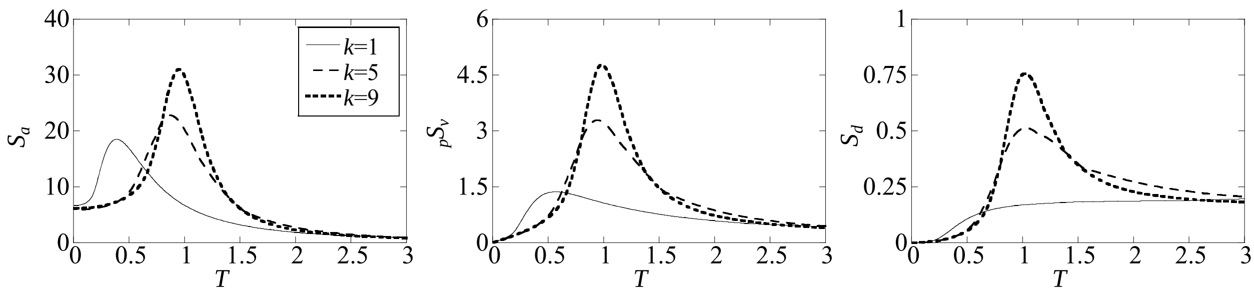

(a) S_a (b) $_pS_v$ (c) S_d

Fig. 2 –Response spectra of Gabor wave (V=1, T_H =1, h=0.05)

3. Proposal of simplified characterization method

In this section, we propose a simplified characterization method for pulse-like ground motions. In the characterization method of this paper, pulse characteristic parameters related to a period, an amplitude, and a duration time are obtained by using pseudo-velocity response spectra $_pS_v$ (h, T) of ground motions. This method can determine the characteristic parameters without performing integration or filtering to the ground motions.

The procedure of the simplified characterization method is described below. The deriving process of the evaluation equations is described later in chapter 4.

1) T_p

The pulse period T_p is defined as the period when the pseudo-velocity response spectrum with damping ratio h = 0.05 $_pS_v$ (h = 0.05, T) is the maximum value $_pS_{v\max}$ (h = 0.05).

2) *k*

The wave number *k* is evaluated by Eq. (4).

$$k = \frac{1-\left\{ {}_pS_v(h_1,T_p) / {}_pS_v(h_2,T_p) \right\}^{1/\beta}}{\alpha\left[h_2\left\{ {}_pS_v(h_1,T_p) / {}_pS_v(h_2,T_p) \right\}^{1/\beta} - h_1 \right]} \tag{4}$$

Here, h_1 and h_2 are damping ratios and $h_1 = 0.1$ and $h_2 = 0.01$. The constant α and β are given $\alpha = 3.05$ and $\beta = -0.696$.

3) T_H

The harmonic wave period T_H is evaluated by Eq. (5).

$$T_H = T_p\left(1+\sqrt{1+8/\sigma^2}\right)/2 \tag{5}$$

Here, σ is determined from *k* in Eq. (3).

4) *V*

The velocity amplitude *V* is evaluated by Eq. (6).

$$V = \frac{{}_pS_v(h=0.05,T_p)}{p(k,h=0.05)\cdot\gamma} \tag{6}$$

Here, $p(k, h = 0.05)$ is obtained by substituting $h = 0.05$ and *k* which is obtained in 2) into Eq. (7).

$$p(k,h) = (1+\alpha kh)^{\beta} \tag{7}$$

The γ is obtained by Eq. (8).

$$\gamma = \frac{\sqrt{\pi}\sigma\overline{T}}{2}\cdot\left[\exp\left\{-\left(\left(\overline{T}+1\right)\sigma\right)^2/4\right\}+\exp\left\{-\left(\left(\overline{T}-1\right)\sigma\right)^2/4\right\}\right] \tag{8}$$

Here, $\overline{T}$ is obtained by Eq. (9).

$$\overline{T} = T_H / T_p \tag{9}$$

If there are other peaks in the ${}_pS_v$, repeat the same procedure from 1) to 4).

4. Deriving process of evaluation equations

This chapter shows the deriving process of the evaluation equations proposed in chapter 3.

4.1 *k*

In this section, the deriving process of the evaluation equation for k in Eq. (4) is described.

Figure 3 shows the response spectrum ratio of the damped ${}_pS_v(h, T)$ to the undamped ${}_pS_v(h = 0, T)$ of Gabor wave. Note that T is normalized by T_H at the horizontal axis. The response spectrum ratio around $T / T_H = 1$ decreases as k and h increase in the figures. Therefore, it is found that k can be evaluated by using the response spectrum ratios.

In this paper, the peak ratio $p(k, h)$ is defined as the ratio of the damped ${}_pS_{v\max}(h)$ to the umdamped ${}_pS_{v\max}(h = 0)$. Note that ${}_pS_{v\max}$ is the maximum value of ${}_pS_v$.

The $p(k, h)$ is regressed by Eq. (7) to determine two parameters α and β. Numerical calculation results of the peak ratio of Gabor wave ($T_H = 1$, $V = 1$, $k = 1$ to 15 in increments of 0.1, $h = 0.01$ to 0.2 in increments of 0.01) are used for the regression. The parameters are determined as $\alpha = 3.05$ and $\beta = -0.696$ to minimize the mean square error between $p(k, h)$ and the numerical calculation results.

Figure 4 (a) and (b) show the peak ratio of $h = 0.05$ and $h = 0.1$ to $h = 0$ of the numerical calculation results and the regression equation $p(k, h)$ according to k. As can be seen in the figures, the regression equation is similar to the numerical calculation results. We confirm that the regression equation is also similar to the numerical calculation results of other damping ratios. However, in case of observed ground motions, the undamped response spectra are jagged and the frequencies at the peak value are not stable. Therefore, the response spectra are smoothed by giving a small damping ratio. In this paper, the peak ratio between the damping ratios $h = 0.1$ and $h = 0.01$ is used for the characterization method. Figure 4 (c) shows the peak ratio of $h = 0.1$ to $h = 0.01$ of the numerical calculation results and the regression equation $p(k, h)$ according to k. In the figure, $p(k, h = 0.1) / p(k, h = 0.01)$ are used as the regression equation. As can be seen in the figure, the regression equation can also evaluate the numerical calculation results sufficiently. Note that we choose the damping ratios $h = 0.1$ and $h = 0.01$ because the change of the peak ratio according to k is larger than other combinations of damping ratios.

From the above, Eq. (4) in chapter 3 are derived from Eq. (10) by substituting Eq. (7).

$$ {}_pS_v(h_1, T_p) / {}_pS_v(h_2, T_p) = p(k, h_1) / p(k, h_2) \tag{10} $$

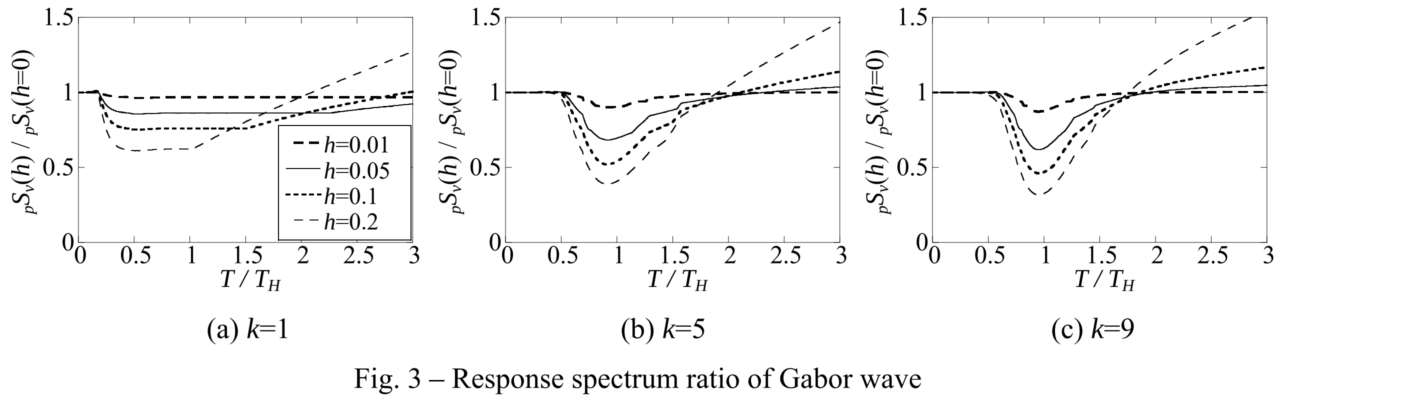

Fig. 3 – Response spectrum ratio of Gabor wave

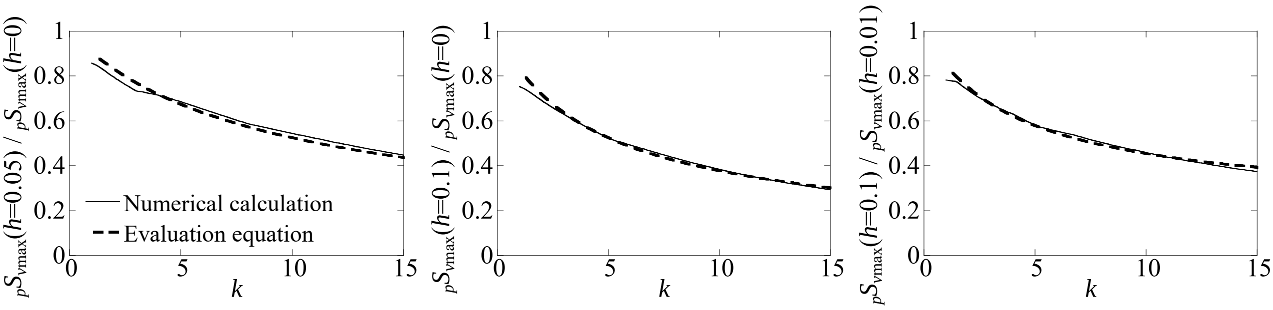

(a) ${}_pS_{vmax}(h{=}0.05)$ / ${}_pS_{vmax}(h{=}0)$ (b) ${}_pS_{vmax}(h{=}0.1)$ / ${}_pS_{vmax}(h{=}0)$ (c) ${}_pS_{vmax}(h{=}0.1)$ / ${}_pS_{vmax}(h{=}0.01)$

Fig. 4 – Relationship between k and response peak ratio of Gabor wave

4.2 T_H

In this section, the deriving process of the evaluation equation for T_H in Eq. (5) is described. This relation has already been derived by Kamei et al [3].

This evaluation equation is derived from the following characteristics of Gabor wave; 1) The predominant period of ${}_pS_v(h, T)$ does not change significantly due to damping ratio h, and 2) The ${}_pS_v$ (h = 0) and the Fourier amplitude of acceleration $|F_a(\omega)|$ correspond with each other around the predominant period.

As a description of 1), Fig. 5 shows the period at ${}_pS_{vmax}$ (h) by numerical calculation of Gabor wave (T_H = 1, V = 1, k = 1 to 15 in increments of 0.1, h = 0, 0.1, 0.05, and 0.1). As can be seen in the figure, the predominant period hardly changes regardless of h. As a description of 2), Fig. 6 shows ${}_pS_v$ (h=0) and $|F_a(\omega)|$ of Gabor wave (T_H = 1, V = 1, k = 5) as an example.

The Fourier amplitude of acceleration of Gabor wave $|F_a(\omega)|$ is theoretically obtained by Eq. (11) and (12).

$$|F_a(\omega)| = \left(\sqrt{\pi} V_p \sigma \bar{\omega} / 2\right) \cdot \left[\exp\left\{ -\left((\bar{\omega}+1)\sigma \right)^2 / 4 \right\} + \exp\left\{ -\left((\bar{\omega}-1)\sigma \right)^2 / 4 \right\} \right] \tag{11}$$

$$\bar{\omega} = \omega / \omega_H = T_H / T \tag{12}$$

The relationship between T_p and T_H is obtained as shown in Eq. (13) to calculate the predominant period from Eq. (11) by neglecting the first term and differentiating the equation.

$$\bar{\omega} = T_H / T_p \approx \left(1 + \sqrt{1 + 8/\sigma^2}\right) / 2 \tag{13}$$

Figure 5 shows a comparison between Eq. (13) and the numerical calculation result. As can be seen in the figure, T_p is evaluated well by Eq. (13). Equation (5) in chapter 3 is obtained by solving Eq. (13) for T_H.

4.3 V

In this section, the deriving process of the evaluation equation for V in Eq. (6) is described. The $p(k, h)$ is used to evaluate V. As described in the previous section, the peak amplitude of the undamped ${}_pS_v$ (h = 0, T) almost coincides with the Fourier amplitude of acceleration $|F_a(\omega)|$. Figure 7 shows a comparison between the numerical calculation result of ${}_pS_{v\max}$ (h = 0) and the result obtained by substituting Eq. (13) into Eq. (11). As can be seen in the figure, ${}_pS_{v\max}$ (h = 0) can be accurately estimated by using Eq. (13) and (11). The evaluation equation of V in chapter 3 consists of the peak ratio of h = 0 and h = 0.05 as shown in Fig. 4 (a) and the equation of the undamped response spectrum is expressed by Eq. (13) and (11). That is, Eq. (6) is equal to the peak ratio of h = 0.05 to h = 0 which is express by Eq. (13) and Eq. (11).

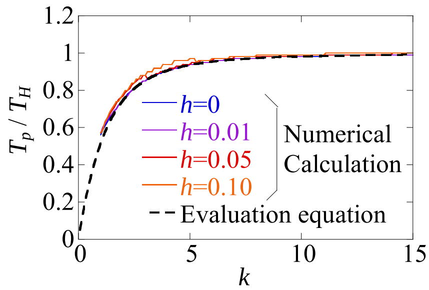

Fig. 5 – Relationship between k and predominat period of ${}_pS_v$ of Gabor wave

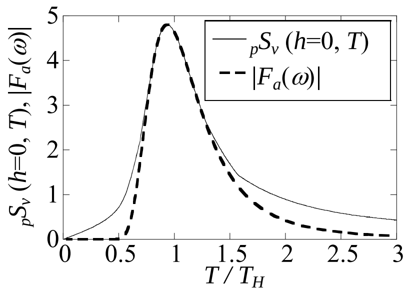

Fig. 6 – $|F_a(\omega)|$ and ${}_pS_v$ (h=0, T) of Gabor wave (k=5)

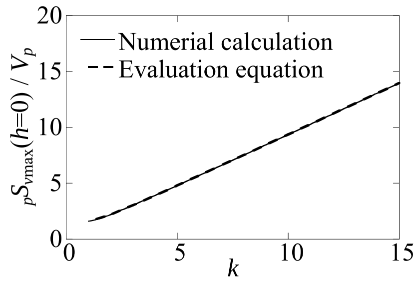

Fig. 7 – Relationship between k and ${}_pS_{v\max}$ (h = 0) of Gabor wave

5. Application examples

In this section, the pulse characteristic parameters of observed pulse-like ground motion are obtained as examples of the characterization method proposed in this paper.

Table 1 shows the observed pulse-like ground motions used in this paper. These ground motions are obtained from NGA West 2 except for 2016 Kumamoto Earthquake. In addition, we also characterize a ground motion observed during the 2016 Kumamoto Earthquake (occurring at 1:25 on April 16).

In this paper, the ground motions of the maximum velocity direction are used for the characterization method as application examples. Although the characterization method in this paper does not require the velocity waveform to determine the pulse characteristic parameters, the velocity waveforms are used to calculate the maximum velocity direction and compare the velocity waveforms of the characterization results. The velocity waveforms provided by NGA West 2 are used except for the 2016 Kumamoto earthquake. For the 2016 Kumamoto earthquake, baseline correction is performed according to [4] and [5]. Table 1 shows the direction of the maximum velocity direction as azimuth which is a clockwise angle from the north.

The characterization method is as described in chapter 3. No filter processing is applied except for the baseline correction performed to Nishihara-mura Komori. For the 1995 Kobe Earthquake Takatori and the 2016 Kumamoto Earthquake Nishihara-mura Komori, the pulse characteristic parameters are calculated from two predominant periods of similar amplitude in ${}_pS_v$ (h = 0.05, T).

Table 1 shows the pulse characteristic parameters obtained in this paper. Figure 8 shows velocity waveform of four ground motions except for two ground motions which have two predominat periods. Note that time of the characterized waves are moved so that time at the maximum velocity of the observed ground motions and the characterized waves become the same. Figure 9 and 10 show ${}_pS_v$ (h = 0.05, T) and S_d (h = 0.05, T) of the characterized waves and observed ground motions. As can be seen in the figures, the characterization is generally performed well. In case of Lucerne, the characterized wave does not able to adequately evaluate the observed spectrum around long period and the displacement response spectrum of the characterized wave underestimates that of the observed ground motion. It is assumed that there are other predominant periods nearby the pulse period we choose in the observed ground motion.

From the above, it is confirmed that the pulse characteristic parameters of the observed ground motion are evaluated easily and uniquely. It is also confirmed that the velocity waveforms and the response spectra of the characterized Gabor wave approximately coincide with those of the observed ground motions.

Table 1 – Results of characterization

Eartthquake	Year	Mw	Station	azimuth (degree)	T_p (s)	T_H (s)	V (cm/s)	k
Imperial Valley	1979	6.5	Meloland	232	2.9	3.1	72	4.4
Landers	1992	7.3	Lucerne	263	4.4	5.1	80	3.1
Northridge	1994	6.7	Rinaldi Receiving Sta.	217	1.1	1.3	132	3.0
Chi-Chi	1999	7.6	TCU068	320	8.6	10.5	257	2.6
Kobe	1995	6.9	Takatori	311	1.3	1.3	127	7.3
					2.1	2.1	113	6.6
Kumamoto	2016	7.0	Nishihara	67	0.8	0.8	100	7.9
					3.1	4.3	199	1.8

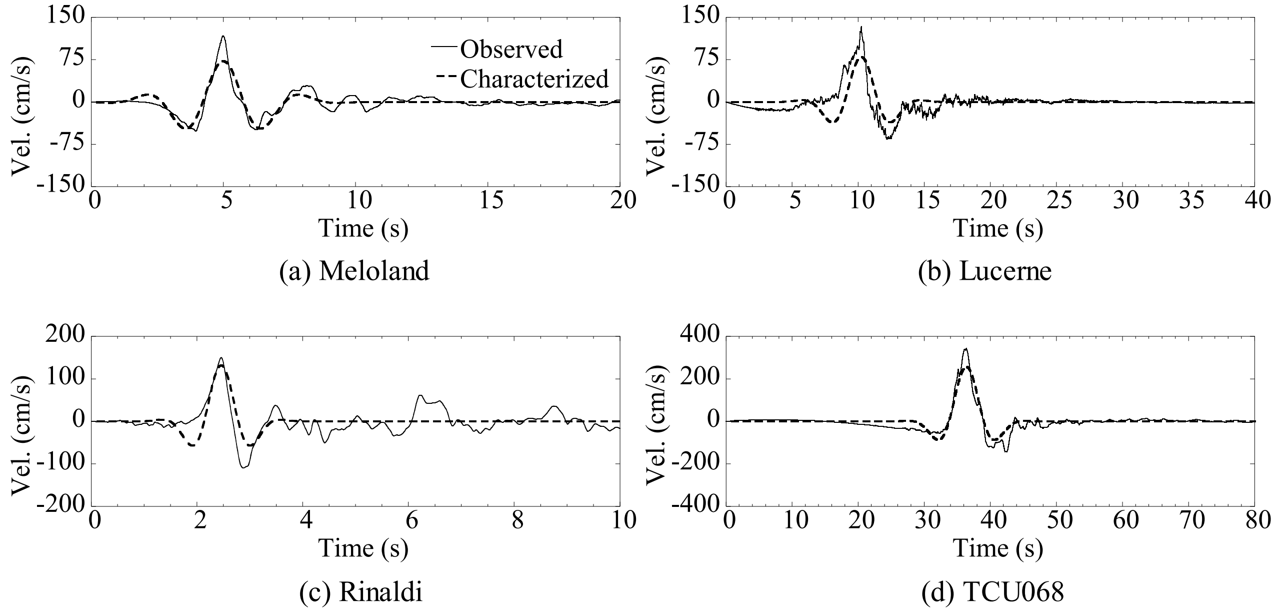

Fig. 8 – Characterization results of velocity waveforms

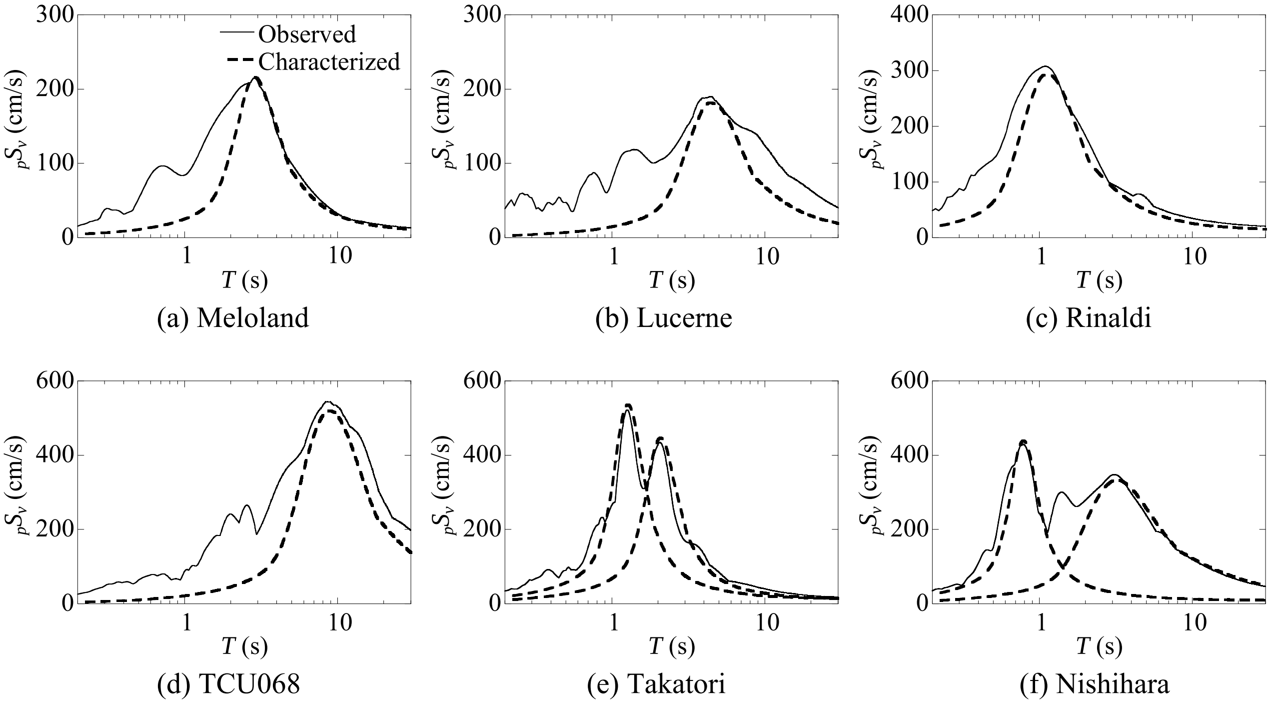

Fig. 9 – Characterization results of $_pS_v\,(h = 0.05, T)$

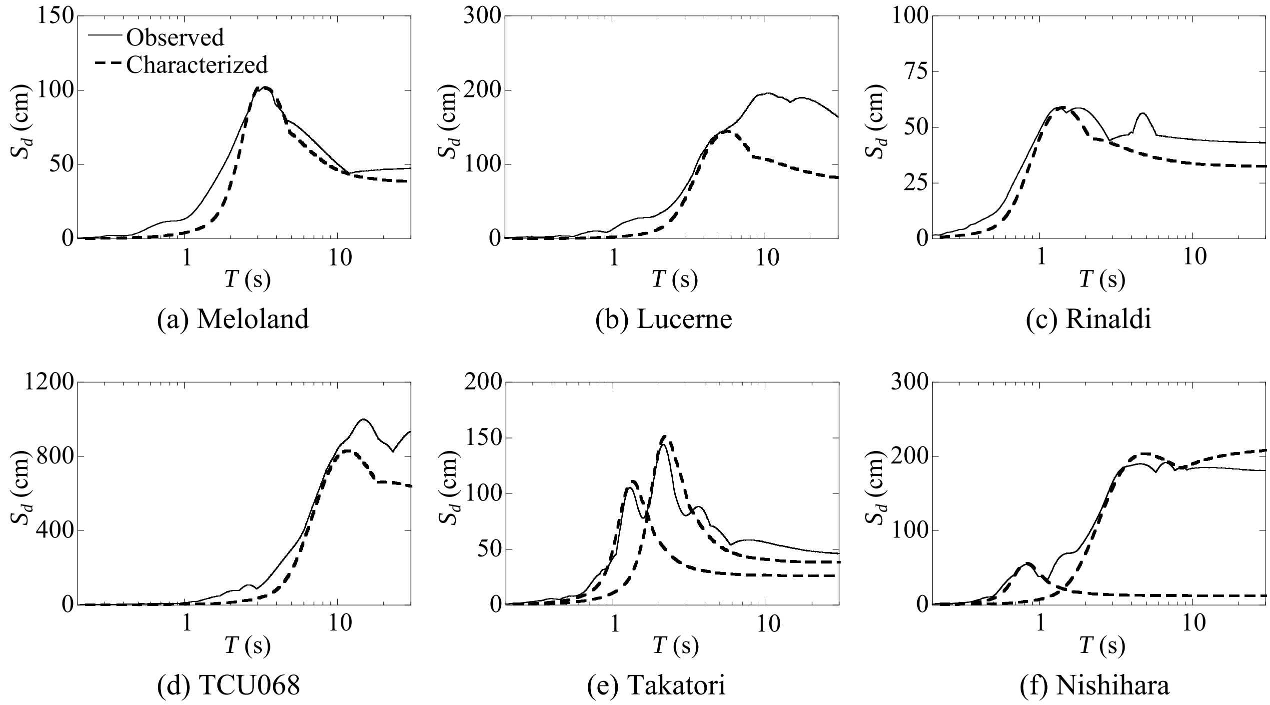

Fig. 10 – Characterization results of $S_d\,(h = 0.05, T)$

6. Conclusions

In this study, we improve the simplified characterization method to use only pseudo-velocity response spectra ${}_pS_v$. In our new proposed characterization method, only the maximum value of the pseudo-velocity response spectra ${}_pS_v$ at different damping ratios and the period at the maximum ${}_pS_v$ of the observed pulse-like ground motions are needed. The pulse characteristic parameters are obtained by substituting the maximum ${}_pS_v$ and the period into the evaluation equations which are proposed in this paper. The evaluation equations proposed in this paper are developed based on the response spectrum characteristics of Gabor wave.

In addition, we apply the characterization method to several typical pulse-like ground motions observed all over the world and calculate the pulse characteristic parameters of the ground motions. It is confirmed that the velocity waveforms and the response spectra of the characterized Gabor wave approximately coincide with those of the observed ground motions.

The advantages of the characterization method proposed in this paper are as follows. Anyone can easily calculate the pulse characteristic parameters as long as the response spectrum is obtained because this method does not use any complicated processing such as calculating momentary input energy as our previous method, integration of accelerations, Fourier transform or Wavelet transform. In this method, the same pulse characteristic parameters can be obtained regardless of users because we do not have to determine the pulse characteristic parameters by trial and error. Furthermore, even for pulse-like ground motions which have several pulse periods such as the ground motions observed during the 2016 Kumamoto earthquake, this method can determine multiple pulse characteristic parameters.

7. Acknowledgements

The authors would like to thank NGA West 2 (Pacific Earthquake Engineering Research Center) and Kumamoto prefectural government for providing ground motion data.

8. References

[1] Sugino M, Murase S, Ohmura S, Hayashi Y (2018): Simplified Characterization of Pulse-like Ground Motions in the 2016 Kumamoto Earthquake. *16th European Conference on Earthquake Engineering*, paper No.10605, Thessaloniki, Greece.

[2] Gabor D (1946): Theory of Communication. Part 1: The Analysis of Information. *Journal of the Institution of Electrical Engineers*, **93** (26), 429-441.

[3] Kamei I, Murase S, Sugino M, Hayashi Y (2018): Pulse Characterization Using Proposed Method and Evaluation of the Response of Buildings for Near-Fault Ground Motions on the 2016 Kumamoto Earthquake, *Journal of Japan Association for Earthquake Engineering*, **18** (1), 18-34. (in Japanese)

[4] Boore D M (2001): Effect of Baseline Corrections on Displacements and Response Spectra for Several Recordings of the 1999 Chi-Chi, Taiwan, Earthquake. *Bulletin of the Seismological Society of America*, **91** (5), 1199-1211.

[5] Murase S, Ohmura S, Sugino M, Hayashi Y (2018): Relationship between Characteristics of Ground Motions and Ratio of Collapsed Wooden Houses in the 2016 Kumamoto Earthquake, *Journal of Japan Association for Earthquake Engineering*, **18** (2), 147-165. (in Japanese)

